

On the mesoscale monitoring capability of Argo floats in the Mediterranean Sea

Antonio Sánchez-Román¹, Simón Ruiz¹, Ananda Pascual¹, Baptiste Mourre² and Stéphanie Guinehut³

¹ IMEDEA (CSIC-UIB), Mallorca, Spain

² SOCIB, Mallorca, Spain

³ CLS, Toulouse, France

Correspondence to: Antonio Sánchez-Román (asanchez@imedea.uib-csic.es)

Abstract

In this work a simplified Observing System Simulation Experiment (OSSE) approach is used to investigate which Argo design sampling in the Mediterranean Sea would be necessary to properly capture the mesoscale dynamics in this basin. The monitoring of the mesoscale features is not an initial objective of the Argo network. However, it is an interesting question in the perspective of future network extensions in order to improve the ocean state estimates. The true field used to conduct the OSSEs is provided by a specific altimetry gridded merged product for the Mediterranean Sea. Synthetic observations were obtained by sub-sampling the Nature Run according to different configurations of the ARGO network. The observation errors required to perform the OSSEs were obtained through the comparison of Sea Level Anomalies (SLAs) from altimetry and Dynamic Height Anomalies (DHAs) computed from the real in-situ Argo network. This analysis also contributes to validate satellite SLAs with an increased confidence. The comparisons have been focused on the sensitivity to the reference level (400 dbar or 900 dbar) used in the computation of the Argo dynamic height. We found that the number of Argo profiles reaching 900 m used to compute DHA is almost 6 times smaller than those reaching 400 m. The simulation experiments show that a configuration similar to the current Argo array in the Mediterranean (with a spatial resolution of $2^\circ \times 2^\circ$) is only able to recover the large-scale signals of the basin. Increasing the spatial resolution to nearly 75×75 km, allows to capture most of the mesoscale signal in the basin and to retrieve the SLA field with a RMSE of 3 cm for spatial scales larger than 150 km, similar to those presently captured by the altimetry. This would represent a theoretical reduction of 40 % of the actual RMSE. Such high-resolution Argo array composed of around 450 floats, cycling every 10 days is expected to increase the actual network cost approximately by a factor six.

1 Keywords: Mediterranean Sea, Observing System Simulation Experiment, altimetry errors, in-
2 situ measurements, profiling float, Array design.

3 **1. Introduction**

4 The Mediterranean Sea is a semi-enclosed basin connected with the Atlantic Ocean
5 through the Strait of Gibraltar. It also communicates with the Black Sea through the Turkish
6 Bosphorus and Dardanelles Straits. The Sicily Strait, with a depth around 300 – 400 m, divides
7 the Mediterranean Sea in two sub-basins: the western basin is influenced by the Gibraltar
8 inflow while the eastern basin is driven by winds and the consequently Levantine Intermediate
9 Water (LIW) formation. The basin-scale circulation of the Mediterranean interacts with sub-
10 basin scale and mesoscale processes, then forming a highly variable general circulation. As a
11 result, the Mediterranean Sea is a particularly interesting area since most of the ocean
12 processes that occur in the world ocean also occur in this basin. The Mediterranean can be
13 considered as a reduced scale ocean laboratory, where processes can be characterized with
14 smaller scales than in other ocean regions [Malanote—Rizoli *et al.*, 2014]. The internal Rossby
15 Radius of deformation in the basin is $O(10\text{—}15 \text{ km})$, which is four times smaller than typical
16 values for much of the world ocean according to Robinson *et al.* [2001]. This fact promotes
17 that in the Mediterranean Sea the spatial resolution of the lagrangian profiling floats of the
18 Argo programme, which consists of a global network of more than 3000 operating floats
19 [Roemmich *et al.*, 2009; Riser *et al.*, 2016] drifting with less than 3 degrees mean spacing,
20 should be reduced four times compared to the open ocean.

21 The Argo programme is a major component of the Global Ocean Observing System and
22 aims to monitor the changing temperature and salinity fields in the upper part of the ocean
23 [Riser *et al.*, 2016]. The majority of the profiling floats used in Argo are programmed to drift at
24 a nominal depth (known as the parking depth) of 1000 m [Riser *et al.*, 2016]. They collect
25 temperature and salinity data every 10 days from the upper 2000 m of the world oceans in
26 order to observe the slow evolution of the large-scale ocean structure.

27 Argo data complement satellite altimetry. The combination of in-situ Argo data with Sea
28 Surface Height (SSH) anomalies derived from satellites allows us to construct time series of the
29 dynamical state of the ocean circulation [Riser *et al.*, 2016]. Altimetry resolves the mesoscale
30 thanks to a finest spatio-temporal sampling. Nevertheless, even though SSH estimates are
31 becoming more precise, the uncertainty associated with altimeter measurements and the
32 geophysical altimeter corrections applied in the SSH computation remains relatively high

1 [Ablain *et al.*, 2009; Couhert *et al.*, 2014; Legeais *et al.*, 2014; Rudenko *et al.*, 2014]. For this
2 reason, some external and independent measurements provided by in-situ observations and
3 numerical models are required to calibrate and validate the altimeter Sea Level Anomaly (SLA)
4 data. These comparisons allow us to obtain the altimetry errors relative to the external
5 measurements and provide an improved picture of SSH that can be used for global and
6 regional studies.

7 At present, Argo data are systematically used together with altimeter data to describe and
8 forecast the 3D ocean state, for ocean and climate research and for sea level rise studies [see
9 e.g. Guinehut *et al.*, 2012; Le Traon, 2013]. This fact demonstrates the very strong and unique
10 complementarities of the two observing systems [Le Traon, 2013].

11 The Argo network in the Mediterranean Sea consists presently of around 80 operating
12 floats deployed in the frame of the MedArgo program
13 (<http://nettuno.ogs.trieste.it/sire/medargo/active/index.php>). The specific semi-enclosed
14 morphology with a large fraction of coastal areas, shallow bathymetry and circulation
15 structures of the basin make profilers programmed with the Argo standard global parking
16 depth of 1000 m not appropriate for this program [Poulain *et al.*, 2007]. This is why a parking
17 depth of 350 m was chosen for the Mediterranean basin. The objective was to track the
18 intermediate waters throughout the Mediterranean which are mostly composed by LIW. This
19 water mass is formed during winter convection in the northern Levantine sub-basin being a
20 crucial component of the Mediterranean thermohaline “conveyor belt” circulation [Poulain *et*
21 *al.*, 2007]. According to the small radius of deformation of the Mediterranean compared with
22 the open ocean at the same latitude, the current number of operating floats in the basin
23 (equivalent to an average spatial resolution of around 2 degrees) improves the global coverage
24 of the Argo network. Nonetheless, it is not enough to properly capture the significant
25 mesoscale circulation features of the basin.

26 The aim of this paper is to investigate which Argo design sampling in the Mediterranean
27 Sea is necessary to recover the mesoscale signal as seen by altimetry. The monitoring of the
28 mesoscale structures is not an initial target of the Argo network [Riser *et al.*, 2016]. However,
29 this is an interesting question in the perspective of future network extensions in order to
30 improve ocean state estimates. Actually, the Argo Steering Team has recently provided a
31 roadmap for how the Argo mission might expand in the near future [Riser *et al.*, 2016].
32 According to these authors, one of the proposed projects is to support an increase in the
33 spatial sampling resolution in particular areas of the word ocean. The objective is the

1 improvement of our view of the complex structure of oceanic variability at spatial scales lesser
2 than the climate scale.

3 To accomplish the proposed aim, we conduct several Observing System Simulation
4 Experiments (OSSEs) in the basin. OSSEs provide a methodology to evaluate and design
5 optimum sampling strategies in ocean observing systems (OOS) [Alvarez and Mourre, 2012].
6 Usually, the method consists in considering the outputs of an ocean model simulation of the
7 area monitored by the OOS as “truth.” Virtual observations from different ocean observing
8 platforms in the OOS are then simulated from the model run and analysed in the same manner
9 than real data [e.g. Alvarez and Mourre, 2012]. OSSEs have been used in oceanography to
10 analyse the impact of different components of the global OOS for ocean analysis and
11 forecasting (see e.g. Oke and Schiller [2007]; Guinehut *et al.* [2012]; Alvarez and Mourre
12 [2012]; Ninove *et al.* [2015]; Oke *et al.*, [2015a] or Oke *et al.*, [2015b]). Here a slightly different
13 approach will be followed with the “truth” being provided by a specific altimetry gridded
14 merged product for the Mediterranean Sea and not by an ocean model simulation. This
15 approach is similar to the one followed by Pascual *et al.*, [2009]. These authors evaluated the
16 quality of global real-time altimetric products by comparing them with independent in-situ tide
17 gauges and drifter data. Moreover, our procedure does not include the validation of the
18 outcomes of the OSSEs against a reference Observing System Experiment (OSE) using real data
19 [Hoffmann and Atlas, 2016]. Thus, our approach can be qualified as a simplified OSSE. This
20 study will assess the scales covered by altimetry which are larger than 100 km [Pujol and
21 Larnicol, 2005]. Notice that the scales mentioned in this paper allude to a definition based on
22 the diameter of individual structures, usually referred to as “feature scales”.

23 The paper is organized as follows: the datasets are described in Section 2. Section 3 details
24 both the processing sequence developed to compare the altimeter data with Argo in-situ
25 measurements and the quantification of the differences between Argo – SLA. These
26 differences are needed to conduct the OSSEs. Thus, a quality assessment of the performances
27 of the altimeter product in the Mediterranean Sea is performed in the first part of this study.
28 The method used here to evaluate the altimeter data is based on the comparison of SLAs from
29 altimetry and Dynamic height Anomalies (DHAs) computed from the in-situ Argo network.
30 Section 4 is devoted to the experiments conducted to recover the SLA fields in the basin from
31 the different configurations of the simulated Argo arrays. Finally, discussion and suggestions to
32 the Argo community regarding future prospects of the in-situ network in the Mediterranean
33 Sea are given in Section 5.

1 **2. Datasets**

2 **2.1 ARGO dataset**

3 We use delayed mode quality-controlled T/S profiles from 2003 to middle 2015 as
4 obtained from the Coriolis Global Data Assembly Centre (www.coriolis.eu.org, ARGO GDAC
5 global distribution database) in the Mediterranean Sea (Figure 1). Dynamic Height (DH) was
6 computed at 5 m depth as an integration of the pressure, temperature and salinity vertical
7 profiles through the water column using a reference level at 400 dbar and 900 dbar (close to
8 400m and 900m, respectively). The choice of these reference levels is conditioned by the
9 availability of the climatology used to compute DH anomalies. This issue will be addressed
10 later. An additional quality control criterion relative to both the profile's position and the
11 pressure, temperature and salinity measurements was applied: only profiles with a quality
12 position flag of 1 (good data) were employed. Moreover, data exhibiting temperature and/or
13 salinity flags different from 1 were removed before the DH computation. As a result of this
14 additional quality check, 194 Argo floats and about 17000 T/S profiles distributed over almost
15 the whole Mediterranean basin are available to compute DH. Their deployment's temporal
16 evolution is shown in Figure 2. More than 90 floats and almost 9000 profiles have been
17 deployed in the last three years of the period investigated. They represent more than 50 % of
18 the Mediterranean Argo network. Actually, the number of both floats and profiles has been
19 systematically increasing from 2008 until 2015 reaching its maximum value in 2014 (36 floats
20 deployed and nearly 4000 profiles carried out).

21 To calculate a consistent DHA with the altimeter SLAs, we use a mean dynamic height as a
22 reference computed through a synthetic climatology approach [Guinehut *et al.*, 2006]. The
23 method to compute the synthetic climatology described in *Guinehut et al.* [2006] consists in
24 the combination of altimeter SLA with simultaneous in-situ dynamic height in order to
25 compute a mean dynamic height, which is referred to the time period spanning from January
26 2003 to December 2011. This climatology presents a global coverage and it has been recently
27 used by *Legeais et al.* [2016] to analyse global altimetry errors by using Argo and GRACE data.
28 In this paper we will test the mean dynamic height computed in the Mediterranean Sea at 400
29 dbar and 900 dbar to estimate DHAs.

30 **2.2 Altimeter measurements**

31 Radar altimeters provide SSH measurements that are not directly comparable with in-situ
32 measurements. Therefore, they must be first referenced and corrected from geophysical

1 signals in order to determine SLAs. In this work, we use SLAs obtained from SSALTO/DUACS
2 multission (Saral, Cryosat-2, Jason-1, Jason-2, T/P, Envisat, GFO, ERS-1, ERS-2, and Geosat)
3 specific reprocessed gridded merged product (level 4) for the Mediterranean Sea. This product
4 is available in the Mean Sea Level Anomaly (MSLA) section of the Archiving, Validation and
5 Interpretation of Satellite Oceanographic website (AVISO, <http://www.aviso.altimetry.fr>). It
6 has been computed with respect to a twenty-year mean referred to the period 1993 – 2012. A
7 comprehensive description of SSALTO/DUACS is given in *Pujol et al.* [2013] and *Pujol et al.*
8 [2016]. The spatial resolution of the dataset is $\frac{1}{6}^\circ \times \frac{1}{6}^\circ$ and the time period used in this work
9 spans from January 1993 to December 2014. The quality of this product can be estimated
10 among others by comparison with in-situ Argo data. Notice that the availability of altimetry
11 and Argo data does not match. Therefore, a common period spanning the period from January
12 2003 (beginning of the Argo dataset) to December 2014 (ending of the altimetric data analysed
13 in this study) has been used in both datasets. Moreover, to perform this comparison, it is
14 critical that altimetry and Argo data have the same interannual temporal reference [*Legeais et*
15 *al.*, 2016]. We estimate DHAs from Argo data through a synthetic mean Argo dynamic height
16 referred to the time period between 2003 and 2011. Thus, the temporal reference of the
17 altimeter SLA must be adapted to this time period. To do that, we subtract the mean of
18 altimetric SSALTO/DUACS maps over 2003 – 2011 from the original SLA time series [*Valladeau*
19 *et al.*, 2012]. On the other hand, the physical content captured by altimetry and Argo profiles
20 is not precisely the same [*Dhomps et al.*, 2011] because the barotropic and the deep steric
21 (deeper than the reference level of the Argo DHA) contributions are missing from the Argo
22 measurements. Therefore, the comparison of altimeter SLA and in situ Argo DHA is used to
23 detect relative anomalies in altimeter data and not absolute bias [*Valladeau et al.*, 2012]. This
24 comparison allows us to obtain a total error estimate including both the instrument and the
25 representation errors which are needed to perform the OSSEs. Representation error can be
26 defined as the component of observation error due to unresolved scales and processes [*Oke*
27 *and Sakov*, 2008].

28 **3. Error estimates from comparison of Argo dynamic heights and** 29 **altimetry sea level anomalies**

30 This section focuses on the comparison of altimetry data with Argo dynamic height in
31 order to estimate the differences between Argo DHA and altimeter SLA needed to specify
32 observation errors in our OSSEs. In addition, this analysis can contribute to validate satellite
33 SLAs with an increased confidence. A sensitivity analysis of the method of comparison of both

1 datasets is provided. This analysis mainly focuses on the impact of the reference depth
2 selected in the computation of the Argo DH on the comparison with specific altimetric SLA
3 gridded merged product for the Mediterranean Sea.

4 **3.1 Method for comparing Altimetry and in-situ Argo data**

5 The comparison method of altimetry with Argo data consists in co-locating both types of
6 datasets since spatial and temporal sampling of altimetry and Argo data are different
7 [Valladeau *et al.*, 2012]. Altimeter grids and synthetic climatologies were spatially and
8 temporally interpolated at the position and time of each in situ Argo profile, which is
9 considered as reference, by using a mapping method based on an optimal interpolation
10 scheme. This considerably reduces errors due to different sampling characteristics of altimeter
11 and in-situ data. As mentioned before, the period investigated extends from January 2003 to
12 December 2014. Then, statistics analyses are performed between both datasets. Co-located
13 altimeter and Argo DH differences are analysed in terms of the standard deviation (STD) for
14 the two reference levels used to compute DHAs from the Argo profiles (namely 400 and 900
15 dbar). In addition, the robustness of the results was investigated by computing means of a
16 bootstrap method with 10^3 random samples taken from the original SLA-DHA series (see
17 details of the method in *Efron and Tibshirani* [1993]). The studies conducted include: (i) the
18 assessment of the method of comparison between Altimetry and Argo data in the
19 Mediterranean Sea; and (ii) the evaluation of the impact of the reference depth selected in the
20 computation of the Argo dynamic height.

21 **3.2 Sensitivity to the reference depth for the integration of the Argo dynamic height**

22 The integration of the Argo T/S profiles for the computation of the in-situ dynamic heights
23 requires a reference level (pressure) where null horizontal velocities are assumed [Legeais *et*
24 *al.*, 2016]. As a rule, the deeper the reference level, the more information from the T/S profiles
25 is considered. This implies a deep sampling of the steric signal through the water column.
26 However, a lower number of vertical profiles (those that reach the reference level) are used in
27 the computation. On the contrary, shallower reference levels allow us to use more floats,
28 although the vertical steric signal will be less sampled. Thus, we aim at determining the
29 impacts of a given reference depth of integration on the Argo spatial sampling and on the
30 comparison with altimeter data in the Mediterranean basin.

31 As it was aforementioned, the choice of a deep reference level for Argo DHAs provides a
32 better estimation of the baroclinic signal. This is more in agreement with the observed signal

1 by altimetry [Legeais *et al.*, 2016]. Therefore, we conduct the analysis on DH comparison
2 computed from Argo data referred to the deeper available reference depth of 900 dbar (nearly
3 900 m) and the specific altimetry product for the Mediterranean Sea. Results are reported in
4 Table 1. The number of T/S Argo profiles used to compute DH (those that reach at least 900 m
5 depth) was 416, corresponding to 23 floats. The standard deviation of the differences between
6 DH from altimetry and Argo (SLA minus DHA) for the common period investigated (from
7 January 2003 to December 2014) was 5.31 cm. It is equivalent to more than 95 % of SLA signal
8 variance. The correlation between both datasets was 0.80.

9 In order to study the impact of the reference level, we repeated the analysis using the
10 shallower reference level of 400 dbar (almost 400 m) for the Argo anomalies but using the
11 same array of Argo profiles reaching 900 m. Now, 24 floats and 479 profiles are available to
12 compare with altimetry due to the synthetic climatology used to compute DHA referred to 900
13 dbar (see Table 1). Nonetheless, we kept the same number of floats and profiles than in the
14 previous computation in order to make both results comparable. The standard deviation of the
15 differences between SLA and DHA referred to 400 dbar computed from profiles spanning until
16 900 m depth was 5.04 cm (see Table 1). It represents an improvement of nearly 10 % in terms
17 of signal variance with respect to the STD diff. computed from Argo DHA referred to 900 dbar
18 (5.31 cm). Moreover, the correlation coefficient increased from 0.80 to 0.82. This is an
19 unexpected outcome since the larger thickness of the water column integrated in the former
20 should promote a lower value of STD. A possible explanation will be done in Section 5.

21 These results (also confirmed from the bootstrap analyses) show that in the
22 Mediterranean basin, it will be advisable to compare SLA from altimetry with DHA from in-situ
23 Argo data referred to 400 dbar. Consequently, DHA referred to 400 dbar was recomputed but
24 using all the available profiles reaching 400 m depth. Now, the number of T/S Argo profiles
25 used to compute DH increased to 2258, thus corresponding to 41 Argo floats. Notice that this
26 more comprehensive number of Argo profiles is almost 6 times larger than the profiles used to
27 compute DHAs referred to 900 dbar. The standard deviation of the differences of SLA – DHA
28 was 4.92 cm while the correlation between both datasets decreased to 0.76. In the framework
29 of our OSSE, this STD value can be considered as an error estimate of the Argo DHA with
30 respect to altimeter SLA in the Mediterranean Sea for the time period investigated.
31 Furthermore, this result represents an improvement of 14 % in terms of signal variance with
32 respect to the one obtained from the differences between SLA and DHA referred to 900 dbar.

33

1 **4- Impact of the number of Argo floats on the reconstructed SLA fields**

2 In this section we aim to investigate which configuration in terms of spatial sampling of the
3 Argo array in the Mediterranean Sea will properly reproduce the mesoscale dynamics in this
4 basin, which is comprehensively captured by new standards of specific altimeter products for
5 this region. To do that, several OSSEs have been conducted to simulate the Argo observing
6 system in the Mediterranean assuming altimetry data computed from specific reprocessed
7 gridded merged product for the basin as the “true” field. As most of the ocean OSSEs
8 conducted to date, OSSEs performed here do not follow the comprehensive design criteria and
9 validation methodology developed for the atmosphere [Halliwell *et al.*, 2014]. Rigorous OSSE
10 procedure includes the validation against a corresponding OSE to guarantee the reliability of
11 the outcomes of the OSSEs [Hoffmann and Atlas, 2016]. As a consequence, our approach can
12 be qualified as simplified OSSE. Further validation will be needed in the future implementing a
13 comprehensive OSSE system.

14 **Experiments design**

15 This section describes the different elements of the OSSEs conducted in the Mediterranean
16 Sea. A flow chart of the methodology developed in provided in Figure 3. The specific altimetry
17 gridded merged product for the Mediterranean Sea, described in section 2.2, has been used as
18 the Nature Run (NR) component of the OSSEs. Namely, we use daily SLA maps along 2014. The
19 region considered covers the entire Mediterranean basin. The original altimetry dataset has a
20 spatial resolution of $\frac{1}{8}^\circ \times \frac{1}{8}^\circ$ and presents 17283 grid points (see Table 2). We obtain synthetic
21 observations from the Nature fields by sub-sampling the NR with the different spatial
22 resolutions displayed in Table 2. The aim is to reproduce some possible configurations of the
23 Argo array network in the Mediterranean Sea. The stations (grid points) associated with each
24 sub-sampled field (figures not shown) will simulate the positions of the Argo floats over a
25 regular grid.

26 In addition, the synthetic observations (re-gridded daily SLA maps) were perturbed
27 simulating realistic observation errors. The differences between altimeter SLA and real Argo
28 DHA directly provide the observation errors in our particular OSSE experiment where Argo
29 DHA are the observations and altimeter SLA is the true field.

30 A random noise generated from a normal distribution function representing the errors
31 characterized in Section 3 but limited to the year 2014 is added to the values of the synthetic
32 observations. The STD difference for the year 2014 is 4.79 cm. Seven experiments were

1 conducted to reconstruct the 2-D SLA fields (sub-sampled daily SLA fields) in the
 2 Mediterranean along 2014 with a spatial resolution of $\frac{1}{3}^\circ \times \frac{1}{3}^\circ$ by applying the Optimal
 3 Interpolation (OI) technique. The parameters used for the computation of the reconstructed
 4 fields were the following: (i) the first guess used to obtain the statistically null-mean residuals
 5 was computed by fitting a polynomial of degree 1. This first guess will be subsequently added
 6 after the computation to recover the total daily field; (ii) the filtering scale was set to be twice
 7 over the spatial distance between stations (according to the box size used in each experiment).
 8 Table 2 summarizes the filtering scale used to compute the recovered SLA fields in the
 9 different reconstructions; (iii) the spatial scale of correlation between stations was determined
 10 from a Gaussian correlation curve computed as follows:

$$11 \quad W = e^{-d^2/2S^2} \quad (1)$$

12 where d is the mean distance between stations and S the spatial scale of correlation. In order
 13 to determine the more suitable spatial scale of correlation for the Mediterranean basin we
 14 computed the correlation curve W for spatial scales varying from 15 km to 50 km. The mean
 15 distance between stations ranged between 0 km and 100 km. Then we compared these
 16 correlation curves with the one obtained for altimetric data computed for the same distances
 17 between stations as follows:

$$18 \quad COR(x) = [1 + ar + \frac{1}{6}(ar)^2 - \frac{1}{6}(ar)^3]e^{-ar} \quad (2)$$

19 with $r = x/L$ and $a = 3.337$; where x is the spatial coordinate of the studied point, and L is the
 20 zonal correlation scale (km) of the Mediterranean basin (100 km). The reader is referred to
 21 *Pujol and Larnicol* [2005] for a more detailed description of this computation. Figure 4 shows
 22 the correlation curve computed for the altimetric data from Eq. (2) and the best fitting curve
 23 obtained from Eq. (1), which corresponds to a spatial correlation scale of 40 km. Therefore, the
 24 S parameter was set to 40 km in all the experiments. (iv) the last parameter to include in the
 25 experiments is the noise to signal variance ratio (γ), defined as the ratio between the Argo
 26 error and the altimetry variance. The former can be established as the variance of the
 27 differences between SLA and DHA in the Mediterranean. This parameter is estimated from the
 28 standard deviation of SLA-DHA differences (4.79 cm) computed for 2014. As a result, we obtain
 29 $\gamma=0.85$ as the true value for the datasets used here (see further details about this parameter in
 30 *Gomis et al.* [2001]).

31 Finally, the retrieved daily SLA maps for 2014 were compared to the NR (also interpolated
 32 to a spatial resolution of $\frac{1}{3}^\circ \times \frac{1}{3}^\circ$) in order to compute the root mean square errors (RMSE)

1 associated with the recovered maps from the sub-sampled fields. This procedure will let us
2 establish the spatial resolution that better captures the mesoscale dynamics in the
3 Mediterranean with a feasible number of stations simulating the locations of Argo floats.

4 **4.1 Impact of the grid box size on analysed SLA fields**

5 In this section we will discuss the impact of the spatial resolution of the synthetic
6 observations (sub-sampled SLA fields) on the retrieval of mesoscale signals in the
7 Mediterranean basin. As a previous step, the RMSE obtained for the seven experiments will be
8 analysed. The 2014 yearly mean values of the RMSE associated with the altimetry maps
9 recovered from the different sub-sampled fields and their annual variability are displayed in
10 Figure 5. Maximum mean RMSE larger than 4 cm (equivalent to 79 % of SLA signal variance)
11 are obtained for the maps recovered from the sub-sampled field reproducing the current
12 spatial resolution of the Argo array in the Mediterranean ($2^\circ \times 2^\circ$). Therefore, this spatial
13 configuration only retrieves 21 % of SLA signal variance due to a poorer capture of the
14 mesoscale features. These maps also exhibit the larger annual variability. This is an expected
15 result that can be explained by both the challenge of reconstructing the same scale signals
16 with only 69 stations (grid points) and the larger filtering scale (around 450 km) used in the
17 experiment (see Table 2). The mean RMSE of the recovered maps exponentially decays as the
18 box-size of the sub-sampled altimetry fields diminishes and therefore, the number of stations
19 enhances. As a result, the mean RMSE reaches an asymptotic value of 2.4 cm (equivalent to
20 28.7 % of SLA signal variance) for the SLA maps retrieved from the sub-sampled fields with a
21 box-size of $0.4^\circ \times 0.4^\circ$. This configuration is equivalent to 1458 stations and captures 71.3 % of
22 SLA signal variance. The standard deviation of the RMSE follows the same pattern exhibiting a
23 minimum annual variability for this spatial resolution.

24 Figure 6 shows an example of the altimetry maps recovered from the sub-sampled SLA
25 fields on 22nd December 2014. The original SLA field for that day interpolated to a spatial
26 resolution of $\frac{1}{3}^\circ \times \frac{1}{3}^\circ$ is displayed in the uppermost panel for comparisons purposes. Notice
27 that the coarse spatial resolution of the $2^\circ \times 2^\circ$ sub-sampled grid (upper-left panel in Figure 6)
28 prevents us from retrieving the mesoscale features observed in the original map and only the
29 large-scale signals are properly captured. As a consequence, the RMSE associated with this
30 reconstruction which simulates the present Argo array in the Mediterranean is around 4.6 cm.
31 On the contrary, the sub-sampled grids with box-sizes of $0.4^\circ \times 0.4^\circ$ and lower (map not
32 shown) are able to retrieve most of the mesoscale structures of the basin with a RMSE of
33 around 2.6 cm. Nonetheless, the high number of stations required to reconstruct the SLA maps

1 (respectively 1458 and 1915, see Table 2) makes this option unviable. Therefore, it is
2 imperative to reach a compromise between the stations used and the extent of the
3 reconstruction performed. In this case, a reasonable solution would be to reconstruct the SLA
4 field from a sub-sampled grid with a box-size of $0.75^\circ \times 0.75^\circ$. This spatial resolution agrees
5 with the theoretical one for the Argo array in the Mediterranean extracted from the internal
6 Rossby radius of deformation computed for the Mediterranean basin. Also, it allows us to
7 retrieve the most representative mesoscale patterns of the basin, for spatial scales larger than
8 150 km, with a feasible number of Argo floats (450 stations). Moreover, the spatial scales
9 resolved by this configuration simulate the spatial scales captured by the altimetry.

10 **4.2 Sensitivity to the irregular sampling**

11 The experiments conducted above let us recover SLA maps computed from theoretical
12 regular-gridded configurations of the Argo array in the Mediterranean. In this section we aim
13 at retrieving altimetry maps from a realistic configuration of the Argo network by using the
14 actual uneven positions of the Argo floats in the basin. Figure 7.a displays the real positions of
15 the 58 Argo floats operating in the Mediterranean Sea on 22nd December 2014. SLA at each
16 single Argo float position was extracted from the original altimetry map of that day (figure not
17 shown). Then, the SLA field for the whole basin was retrieved by following the procedure
18 applied to the regular-gridded sub-sampled fields.

19 On the other hand, and since the mean number of Argo floats in the Mediterranean is set
20 to around 80, random virtual floats were added to the actual Argo array of that day. The aim
21 was to reach the mean number of platforms normally operating on the basin. The virtual floats
22 were added by using a normal distribution function computed from the mean and standard
23 deviation of the positions of the Argo Array in the Mediterranean. Then, the SLA data was
24 obtained at the locations of both the actual and virtual floats (see Figure 7.b). We kept on
25 adding random virtual floats until reaching an Argo array of 150, 250 and 450 stations. Their
26 locations and the corresponding SLA data extracted at each position are respectively displayed
27 in Figures 7.c, d and e. SLA field for the whole basin was then recovered for each configuration
28 of the Argo array according to the procedure described above. Reconstructed SLA fields were
29 compared with the original altimetry map of that day. Figure 8 summarizes the results
30 obtained from both the uneven and regular-gridded experiments conducted on 22nd December
31 2014. The errors associated with the SLA maps recovered from the different configurations of
32 the Argo array (gray triangles) present a maximum RMSE of nearly 5 cm when only the 58 Argo
33 floats operating that day are used to reconstruct the SLA field. As expected, RMSEs decay as

1 the number of Argo floats increases (notice that here an Argo array configuration with 750
2 floats has been also included in order to have a better overview of their general pattern). This
3 decrease follows the same pattern that the RMSEs obtained from the regular-gridded
4 experiments (black line) although larger values are observed here. This fact is related to the
5 uneven spatial distribution of the Argo platforms in the basin.

6 5- Discussion

7 The Argo network in the Mediterranean Sea consists presently of around 80 operating
8 floats drifting with less than 2 degrees mean spacing. Even though this array improves the
9 global coverage of the Argo network, it only captures the large-scale circulation features of the
10 basin. In this work, we have investigated which configuration in terms of the spatial sampling
11 of the Argo array in the Mediterranean would be necessary to recover the mesoscale dynamics
12 in the basin as seen by altimetry. The monitoring of the mesoscale features is not an Argo
13 program target. However, this issue is of concern since it can help the current ocean state
14 estimates.

15 To do that, we have conducted several Observing System Simulated Experiments (OSSEs) in
16 the basin. We have followed a simplified OSSE approach by contrast to the comprehensive
17 approach including an equivalent Observing System Experiment. Consequently, our results
18 represent a first look that could be further validated in the future with a comprehensive OSSE
19 system. The true field, provided by gridded altimetry maps in this OSSE, was subsampled
20 according to different configurations of the Argo network. The observation errors required to
21 perform the OSSEs were obtained through the comparison of SLAs from altimetry and DHAs
22 computed from the real in-situ Argo network. The comparisons have been focused on the
23 sensitivity to the reference level (400 dbar or 900 dbar) used in the computation of the Argo
24 dynamic height. We found that the number of Argo profiles reaching 900 m used to compute
25 DHA is almost 6 times smaller than those reaching 400 m. Therefore, the choice of the
26 reference depth has repercussion in the number of valid Argo profiles and thus in their
27 temporal sampling and the coverage of the Argo network used to compare with altimeter
28 data. In addition, the computation of the differences between altimetry and Argo data
29 referred to both 400 and 900 dbar revealed a standard deviation of SLA – DHA differences 1.67
30 cm lower (in terms of variance) when computing DHA referred to 400 dbar. This fact, together
31 with both a higher correlation coefficient between both datasets and the larger number of
32 available profiles, suggest to preferably consider the 400 dbar level as reference level to
33 compute DHA from Argo data in the Mediterranean basin. This leads to a standard deviation of

1 the differences between both datasets of 4.92 cm (equivalent to 90 % of SLA signal variance).
2 Conversely, one would expect better results when using 900 dbar as reference level because
3 the physical content (variance) of a larger fraction of the water column is considered when
4 computing Argo DH. However, the more comprehensive number of available Argo profiles
5 when using 400 dbar as reference level, and thus the larger coverage of the Argo network,
6 seems to play a more critical role in the comparisons with altimeter data in the Mediterranean
7 basin than the deep sampling of the steric signal. On the other hand, the climatology used here
8 to compute DHA could be not as accurate at 900 m due the lower number of historical data
9 available at that depth, then resulting in larger standard deviations of the differences between
10 both datasets. Nonetheless, the evaluation of this climatology is out of the scope of this paper
11 and it will be addressed in further investigations.

12 Another interpretation of the results obtained here could be done in terms of the
13 dynamics of the water masses residing in the Mediterranean Sea. Due to the excess of
14 evaporation over precipitation and river run-off, an Atlantic inflow through the Strait of
15 Gibraltar is required to balance the salt and freshwater budgets of the basin. As the Atlantic
16 water spreads into the Mediterranean, it becomes saltier and denser under the influence of
17 intense air-sea interactions [Criado-Aldeanueva *et al.*, 2012]. Most of this flow will return to
18 the Atlantic Ocean as Levantine Intermediate Water (LIW), formed during winter convection in
19 the Levantine sub-basin while another part will be transformed into deep waters along the
20 basin [Criado-Aldeanueva *et al.*, 2012]. The LIW spreads over different fractions of the water
21 column along its path towards the Atlantic Ocean: in the eastern basin it is located between
22 100 – 400 m depth while it spreads between 200 – 700 m approximately in the western basin
23 [Zavatarelli and Mellor, 1995] Therefore, in the eastern Mediterranean the reference level of
24 400 dbar (near 400 m depth) will be close to the interface between this water mass and those
25 residing at deeper levels, which usually have different pathways. As a consequence, velocities
26 around 400 m depth would be significantly reduced as a result of friction while they could be
27 enhanced as we move towards deeper levels fed by the Mediterranean deep water masses. As
28 a result, velocities at 900 m depth could not be close to zero, as we assume in the DHA
29 computation, then promoting coarser results when comparing altimetry with Argo data
30 referred to 900 dbar. In order to check this hypothesis, we recomputed the SLA – DHA
31 differences for the eastern and western basins (see Tables S1 and S2 in the supplementary
32 data). In a first step, the Argo profiles available to compute DH in the whole Mediterranean
33 were sorted out according to their location. We found that 44 % of them were deployed in the
34 western Mediterranean while the remaining 56 % are located in the eastern basin. Then, DHA

1 referred to 400 and 900 dbar was computed and compared with SLA from Altimetry according
2 to the procedure described in section 3. In the eastern Mediterranean, the computation of the
3 differences between altimetry and Argo data referred to both 400 and 900 dbar revealed a
4 standard deviation of SLA – DHA differences 1.88 cm lower (in terms of variance) when
5 computing DHA referred to 400 dbar. This pressure level is located nearby the bounds of the
6 LIW in this region, where velocities close to zero are expected. By contrast, in the western
7 basin we obtained a standard deviation of SLA – DHA differences 1.26 cm lower when
8 computing DHA referred to 900 dbar. This result is consistent with the vertical distribution of
9 the LIW in the western Mediterranean. Furthermore, the depth of the LIW core in most of the
10 Mediterranean basin is also the reason of choosing 350 m as the parking depth for the Argo
11 floats in the Mediterranean [Poulain *et al.*, 2007].

12 Results reported from the regular-gridded experiments have shown that the reconstructed
13 SLA maps from a configuration similar to the current Argo array in the Mediterranean (spatial
14 resolution of $2^\circ \times 2^\circ$) are not able to capture the mesoscale features of the basin. As a
15 consequence, these maps only retrieve 21 % of SLA signal variance. This is an expected result
16 because the initial target of the Argo program is to monitor the large-scale ocean variability.
17 Increasing the resolution, reconstructed SLA fields from a $0.75^\circ \times 0.75^\circ$ grid box of SLA
18 observations retrieve 66 % of SLA signal variance. This reconstruction captures the large-scale
19 signal and most of the mesoscale features of SLA fields in the basin exhibiting a mean RMSE
20 lower than 3 cm (equivalent to 34 % of SLA signal variance). In addition, this spatial resolution
21 agrees with the theoretical one extracted from the internal Rossby radius of deformation
22 computed for the Mediterranean basin. The same outcomes were also obtained from the
23 experiments conducted by using the actual positions of the Argo array in the basin. Here,
24 larger values for the RMSEs of the recovered SLA maps were systematically obtained due to
25 the uneven spatial distribution of the Argo platforms in the basin. However, we must be
26 cautious about these results because the test has been conducted only along one Argo cycle
27 (10 days). Anyway, similar results to the ones obtained here are expected to emerge from
28 longer experiments according to the results obtained from the analysis of 2014 yearly RMSEs
29 associated with the altimetry maps recovered from the different regular-gridded sub-sampled
30 fields.

31 To summarize, and in light of a hypothetical future expansion of the Argo network, this
32 OSSE experiment provides indications that a spatial resolution of nearly 75×75 km would be
33 enough to retrieve the SLA field with an RMSE of 3 cm for spatial scales higher than 150 km,
34 similar to those presently captured by the altimetry. This would represent a theoretical

1 reduction of 40 % of the actual RMSE. Such high-resolution Argo array composed of around
2 450 floats, cycling every 10 days is expected to increase the actual network cost approximately
3 by a factor six. This investment would in turn certainly have significant and positive
4 repercussions on the realism of numerical models that assimilate Argo profiles.

5 **Acknowledgements**

6 The research leading these results has received funding from the European FP7 under the
7 E-AIMS (Euro-Argo Improvements for the GMES Marine Service) project (Code: 312642) and
8 the Sea Level Thematic Assembly Center (SL-TAC) of the Copernicus Marine and Environment
9 Monitoring Service (CMEMS). Argo data are collected and made freely available by the
10 International Argo Program and the national programs that contribute to it
11 (<http://aego.ucds.edu> and www.jcommops.org/argo). Altimetry data are generated, processed
12 and freely distributed by CMEMS (<http://marine.copernicus.eu/>). We gratefully acknowledge
13 the constructive comments by two reviewers, which helped to improve the manuscript.

14

15 **Competing interests**

16 The authors declare that they have no conflict of interest.

17

18

19

20

21

22

23

24

25

26

1 References

2 Ablain, M., Cazenave, A., Valladeau, G., and Guinehut, S. (2009), A new assessment of the error budget
3 of global mean sea level rate estimated by satellite altimetry over 1993–2008, *Ocean Sci.*, 5, 193–
4 201, doi:10.5194/os-5-193-2009.

5 Alvarez, A. and B. Mourre (2012), Optimum Sampling Designs for a Glider–Mooring Observing Network.
6 *Journal of Atmospheric and Oceanic Technology*, Vol. 29, 2012, pp. 601–612.

7 Arnault, S., I. Pujol, and J. L. Melice (2011), In situ validation of Jason-1 and Jason-2 altimetry missions in
8 the tropical Atlantic Ocean. *Mar. Geod.* 34(3–4), Part 2: 319–339.

9 Bouffard, J., A. Pascual, S. Ruiz, Y. Faugère, and J. Tintoré (2010), Coastal and mesoscale dynamics
10 characterization using altimetry and gliders: A case study in the Balearic Sea, *J. Geophys. Res.*, 115,
11 C10029, doi:10.1029/2009JC006087.

12 Couhert, A., Cerri, L., Legeais, J. F., Ablain, M., Zelensky, P., Haines, N. P., Lemoine, B. J., Bertiger, F. G.,
13 Desai, D., and Otten, M. (2014), Towards the 1mm/y stability of the radial orbit error at regional
14 scales, *Adv. Space Res.*, doi:10.1016/j.asr.2014.06.041, online first.

15 Criado-Aldeanueva, F., F. Javier Soto-Navarro and J. Garcia-Lafuente (2012), Seasonal and interannual
16 variability of surface heat and freshwater fluxes in the Mediterranean Sea: budgets and exchange
17 through the Strait of Gibraltar. *Int. J. Climatol.* 32: 286–302 (2012). DOI: 10.1002/joc.2268

18 Dhomps, A.L., S. Guinehut, P.Y. Le Traon, and G. Larnicol (2011), A global comparison of Argo and
19 satellite altimetry observations. *Ocean Science* 7(2): 175–183.

20 Efron, B., & Tibshirani, R. J. (1993), An introduction to the bootstrap. New York: Chapman & Hall/CRC.

21 Escudier, R., J. Bouffard, A. Pascual, P.-M. Poulain, and M.-I. Pujol (2013), Improvement of coastal and
22 mesoscale observation from space: Application to the northwestern Mediterranean Sea, *Geophys.*
23 *Res. Lett.*, 40, doi:10.1002/grl.50324.

24 Gomis, D., S. Ruiz, and M. A. Pedder (2001), Diagnostic analysis of the 3D ageostrophic circulation from a
25 multivariate spatial interpolation of CTD and ADCP data, *Deep Sea Res.*, Part I, 48, 269–295,
26 doi:10.1016/S0967- 0637(00)00060-1.

27 Guinehut, S., Le Traon, P. Y. and Larnicol, G. (2006), What can we learn from Global
28 Altimetry/Hydrography comparisons?, *Geophys. Res. Lett.*, 33, L10604, doi: 10.1029/2005GL025551.

29 Guinehut, S., Dhomps, A.L., Larnicol, G., and Le Traon, P.Y. (2012), High resolution 3-D temperature and
30 salinity fields derived from in situ and satellite observations, *Ocean Sci.*, 8, 845–857, doi:10.5194/os-
31 8-845-2012.

32 Halliwell, G. R., Jr., A. Srinivasan, V. Kourafalou, H. Yang, D. Willey, M. Le Hénaff, and R. Atlas (2014),
33 Rigorous evaluation of a fraternal twin ocean OSSE system for the open Gulf of Mexico. *J. Atmos.*
34 *Oceanic Technol.*, 31, 105–130, doi:10.1175/JTECH-D-13-00011.1.

35 Hoffman, R. N., and R. Atlas (2016), Future Observing Systems Simulation Experiments, *Bull. Amer.*
36 *Meteorol. Soc.*, doi: <http://dx.doi.org/10.1175/BAMS-D-15-00200.1>

37 Legeais, J.F., Ablain, M., and Thao, S. (2014), Evaluation of wet troposphere path delays from
38 atmospheric reanalyses and radiometers and their impact on the altimeter sea level, *Ocean Sci.*, 10,
39 893–905, doi:10.5194/os-10-893-2014.

40 Legeais, J.F., Prandi, P., and Guinehut, S. (2016), Analyses of altimetry errors using Argo and GRACE data,
41 *Ocean Sci.*, 12, 647–662, doi:10.5194/os-12-647-2016.

1 Le Traon, P. Y. (2013), From satellite altimetry to Argo and operational oceanography: three revolutions
 2 in oceanography, *Ocean Sci.*, 9, 901–915, doi:10.5194/os-9-901-2013.

3 Malanotte-Rizzoli, P., Font, J., Garcia-Ladona, E., Pascual, A., Tintoré, J., Triantafyllou, G., (2014), Physical
 4 forcing and physical/biochemical variability of the Mediterranean Sea: a review of unresolved issues
 5 and directions for future research. *Ocean Sci.* 10, 281–322. <http://dx.doi.org/10.5194/os-10-281-2014>.

7 Mitchum, G. T. (1998), Monitoring the stability of satellite altimeters with tide gauges. *J. Atmos. Oceanic
 8 Tech.* 15: 721–730.

9 Mitchum, G. T. (2000), An improved calibration of satellite altimetric heights using tide gauge sea levels
 10 with adjustment for land motion, *Mar. Geod.*, 23, 145–166.

11 Nerem, R. S., D. Chambers, C. Choe, and G. Mitchum, (2010), Estimating mean sea level change from the
 12 TOPEX and Jason altimeter missions. *Mar. Geod.* 33: 435–446.

13 Ninove, F., Le Traon, P. Y., Remy, E., and Guinehut, S. (2015), Spatial scales of temperature and salinity
 14 variability estimated from Argo observations, *Ocean Sci. Discuss.*, 12, 1793-1814, doi:10.5194/osd-
 15 12-1793-2015.

16 Oke P. R. and Sakov P., (2008), Representation error of oceanic observations for data assimilation. *J
 17 Ocean Atmos Technol.* 25:1004–1017.

18 Oke, P. R. and Schiller, A. (2007), Impact of Argo, SST, and altimeter data on an eddy-resolving ocean
 19 reanalysis, *Geophys. Res. Lett.*, 34, L19601, doi:10.1029/2007GL031549.

20 Oke, P. R., G. Larnicol, Y. Fujii; G. C. Smith, D. J. Lea, S. Guinehut, E. Remy, M. A. Balmaseda, T. Rykova, D.
 21 Surcel-Colan, M. J. Martin, A. A. Sellar, S. Mulet and V Turpin, (2015a), Assessing the impact of
 22 observations on ocean forecasts and reanalysis: Part 1, Global studies. *Journal of Operational
 23 Oceanography*, 8:sup1, s49-s62, doi: 10.1080/1755876X.2015.1022067.

24 Oke, P. R., G. Larnicol, E.M. Jones, V. Kourafalou, A.K. Sperrevik, F. Carse, C.A.S. Tanajura, B. Mourre, M.
 25 Tonani, G.B. Brassington, M. Le Henaff, G.R. Halliwell Jr., R. Atlas, A.M. Moore, C.A. Edwards, M.J.
 26 Martin, A.A. Sellar, A. Alvarez, P. De Mey & M. Iskandarani, (2015b), Assessing the impact of
 27 observations on ocean forecasts and reanalyses: Part 2, Regional applications, *Journal of
 28 Operational Oceanography*, 8:sup1, s63-s79, DOI:10.1080/1755876X.2015.1022080.

29

30 Pascual, A., C. Boone, G. Larnicol, and P. Y. Le Traon (2009), On the quality of real-time altimeter gridded
 31 fields: Comparison with in situ data, *J. Atmos. Oceanic Technol.*, 26, 556–569,
 32 doi:10.1175/2008JTECHO556.1.

33 Poulain, P.M., R. Barbanti, J. Font, A. Cruzado, C. Millot, et al. (2007), MedArgo: a drifting profiler
 34 program in the Mediterranean Sea. *Ocean Science*, European Geosciences Union, 2007, 3 (3),
 35 pp.379-395.

36 Pujol, M.I. and Larnicol, G. (2005), Mediterranean Sea eddy kinetic energy variability from 11 years of
 37 altimetric data. *J. Mar. Sys.* 65 (1 – 4):484 – 508.

38 Pujol M.I., Y. Faugère, J.F. Legeais, M.H. Rio, P Schaeffer, E. Bronner, N. Picot (2013), A 20-year reference
 39 period for SSALTO/DUACS products, OSTST, 2013.

40 Pujol M.I., Y. Faugère, G. Taburet, S. Dupuy, C. Pelloquin, M. Ablain, and N. Picot (2016), DUACS DT2014:
 41 the new multi-mission altimeter data set reprocessed over 20 years. *Ocean Sci.*, 12, 1067–1090,
 42 2016. Doi:10.5194/os-12-1067-2016.

43 Riser SC, Freeland HJ, Roemmich D, Wijffels S, Triosi A, Belbéoch M, Gilbert D, Xu J, Pouliquen S,
 44 Thresher A, Le Traon P-Y, Maze G, et al. (2016), Fifteen years of ocean observations with the global
 45 Argo array, *Nat Clim Chang.* 6(2):145-153, <http://dx.doi.org/10.1038/nclimate2872>.

1 Robinson, A.R., Leslie, W.G., Theocaris, A., Lascaratos, A., (2001), Encyclopedia of Ocean Sciences.
2 chap. Mediterranean Sea Circulation vol. 3. Academic, London, pp. 1689–1705.
3 <http://dx.doi.org/10.1006/rwos.2001.0376>.

4 Roemmich, D., and the Argo Steering Team (2009), Argo: the challenge of continuing 10 years of
5 progress. *Oceanography*, 22, 46 — 55, doi: 10.5670/oceanog.2009.65.

6 Rudenko, S., Dettmering, D., Esselborn, S., Schöne, T., Förste, C., Lemoine, J.-M., Ablain, M., Alexandre,
7 D., and Neumayer, K.H. (2014), Influence of time variable geopotential models on precise orbits of
8 altimetry satellites, global and regional mean sea level trends, *Adv. Space Res.*, 54, 92–118,
9 doi:10.1016/j.asr.2014.03.010.

10 Ruiz, S., A. Pascual, B. Garau, I. Pujol, and J. Tintore (2009a), Vertical motion in the upper ocean from
11 glider and altimetry data, *Geophys. Res. Lett.*, 36, L14607, doi:10.1029/2009GL038569.

12 Ruiz, S., A. Pascual, B. Garau, Y. Faugere, A. Alvarez, and J. Tintoré (2009b), Mesoscale dynamics of the
13 Balearic Front, integrating glider, ship and satellite data, *J. Mar. Syst.*, 78, S3-S16, doi:10.1016/j.
14 jmarsys.2009.01.007.

15 Troupin C., A Pascual, G. Valladeau, A. Lana, E. Heslop, S. Ruiz, M. Torner, N. Picot, J. Tintoré (2015),
16 Illustration of the emerging capabilities of SARAL/AltiKa in the coastal zone using a multi-platform
17 approach. *Advances in Space Research* 55-1, p. 51-59. doi:10.1016/j.asr.2014.09.011.

18 Valladeau G., JF Legeais, M. Ablain, S. Guinehut and N. Picot (2012), Comparing Altimetry with tide
19 gauges and Argo Profiling Floats for data quality assessment and Mean Sea Level studies, *Marine
20 Geodesy* Vol. 35 Suppl. 1.

21 Zavatarelli M. and G. L. Mellor (1995), A numerical study of the Mediterranean Sea circulation, *J. Phys.
22 Ocean.* 25, p. 1384 – 1414

23

24

25

26

27

28

29

30

31

32

33

34

35

1

	All valid profiles (DHA ref. 900 dbar)		Profiles reaching 900m (DHA ref. 400 dbar)		All valid profiles (DHA ref. 400 dbar)	
Argo Floats	23		24		41	
Argo Profiles	416		479		2258	
std (SLA-DHA,cm)	5.31	0.20	5.04	0.17	4.92	0.07
R (SLA-DHA)	0.80	0.02	0.82	0.02	0.76	0.01

2

3 Table 1: Comparison of correlation and standard deviation (cm) of the differences between new
 4 AVISO product for the Mediterranean Sea and Argo data referred to both 400 dbar and 900 dbar
 5 (sub-columns on the left). Sub-columns on the right display the results of the robustness
 6 experiments in terms of standard deviations (see text for details). DHA referred to 400 dbar has
 7 been computed for the whole valid Argo profiles and those reaching 900 m depth for
 8 comparison purposes. The number of Argo platforms and vertical profiles used are also showed.

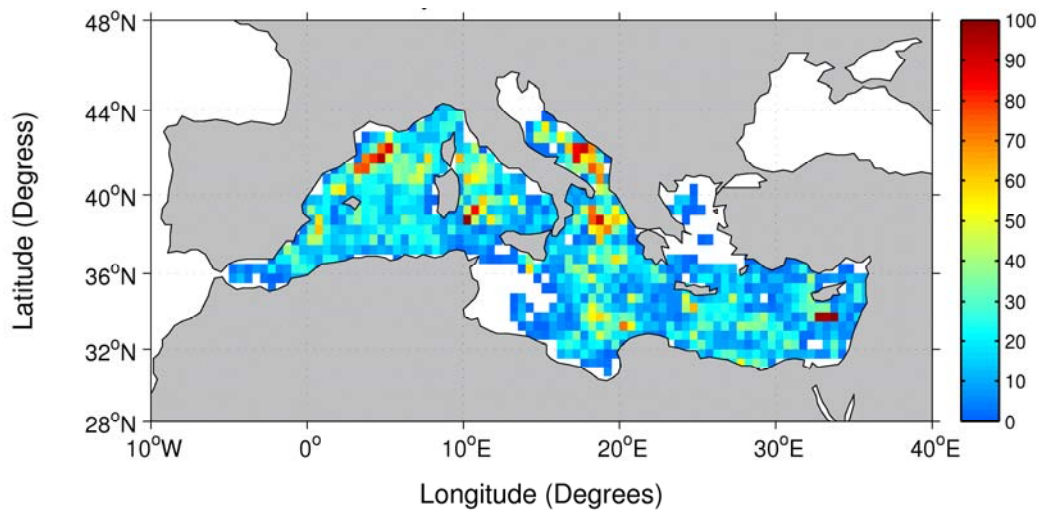
9

Spatial resolution (degrees)	Number of stations	Filtering scale (km)
$2^\circ \times 2^\circ$	69	445
$1.5^\circ \times 1.5^\circ$	121	333
$1^\circ \times 1^\circ$	273	225
$0.75^\circ \times 0.75^\circ$	482	167
$0.5^\circ \times 0.5^\circ$	1082	111
$0.4^\circ \times 0.4^\circ$	1458	95
$0.3^\circ \times 0.3^\circ$	1915	82
$0.125^\circ \times 0.125^\circ$	17283	—

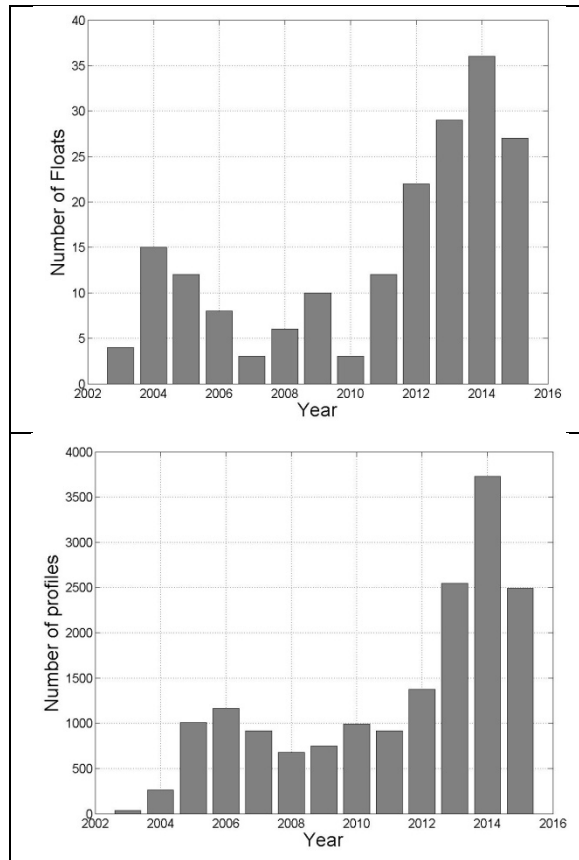
1

2 Table 2: Spatial resolution (degrees) and associated number of stations of the different sub-
 3 sampled fields used to reconstruct the SLA in the Mediterranean. The lower row displays the
 4 spatial resolution and stations of the original altimetry maps. The filtering scale (km) used to
 5 compute the recovered SLA fields in the different reconstructions have been also included.

6



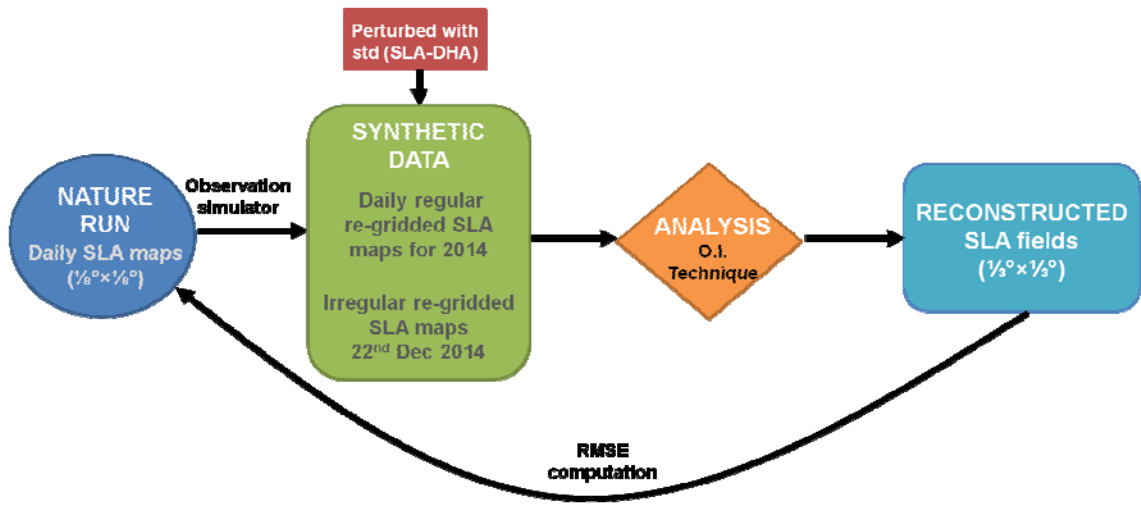
1
2 Figure 1. Number of Argo profiles on boxes of $0.5^\circ \times 0.5^\circ$ of lat-lon performed between 2003
3 and 2015 in the Mediterranean Sea and used to compute Argo DHs. Only profiles with a
4 position quality flag of 1 (good data) have been considered.
5



1

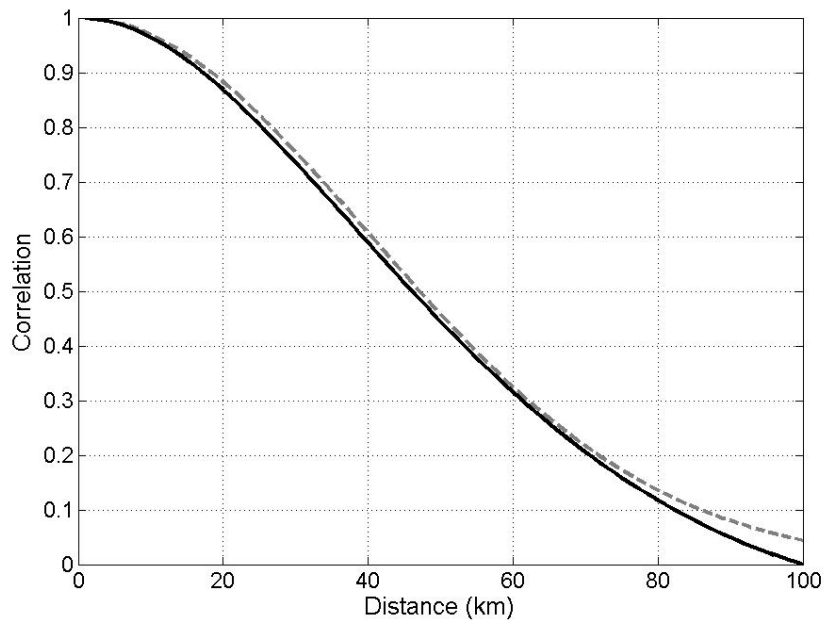
2 Figure 2: Temporal evolution of Argo floats (upper panel) and Argo profiles (lower panel) with
3 a position quality flag of 1 deployed in the Mediterranean Sea since 2003 until the middle of
4 2015.

5



- 1
- 2
- 3 Figure 3: Flow chart showing the elements of the OSSEs conducted for the Mediterranean Sea.
- 4 Datasets used in each component are also indicated.

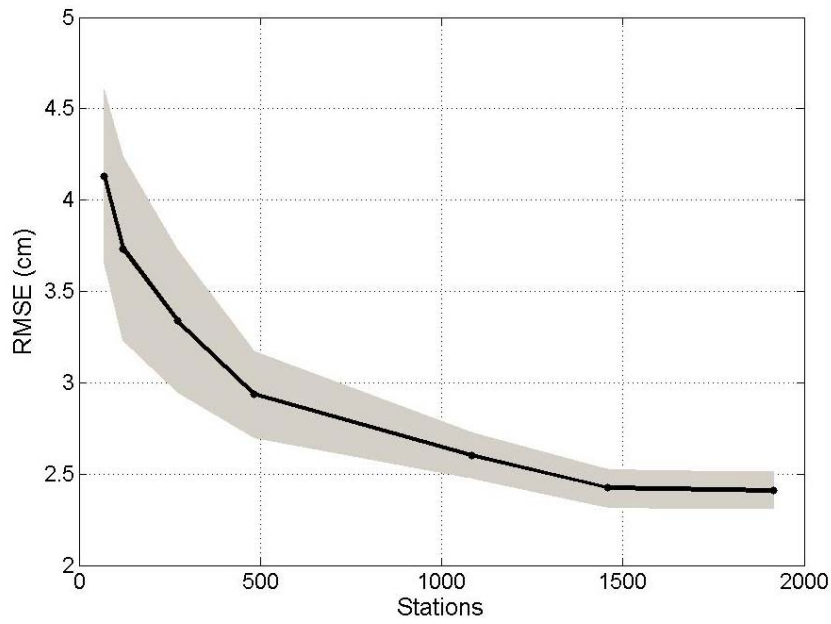
1



2

3 Figure 4: Correlation curve computed for altimetric data (black solid line) for a typical zonal
4 scale of correlation for the Mediterranean region of 100 km. The gray dashed line shows the
5 best fitting correlation curve obtained for the reconstruction experiments. It corresponds to a
6 spatial scale of correlation of 40 km.

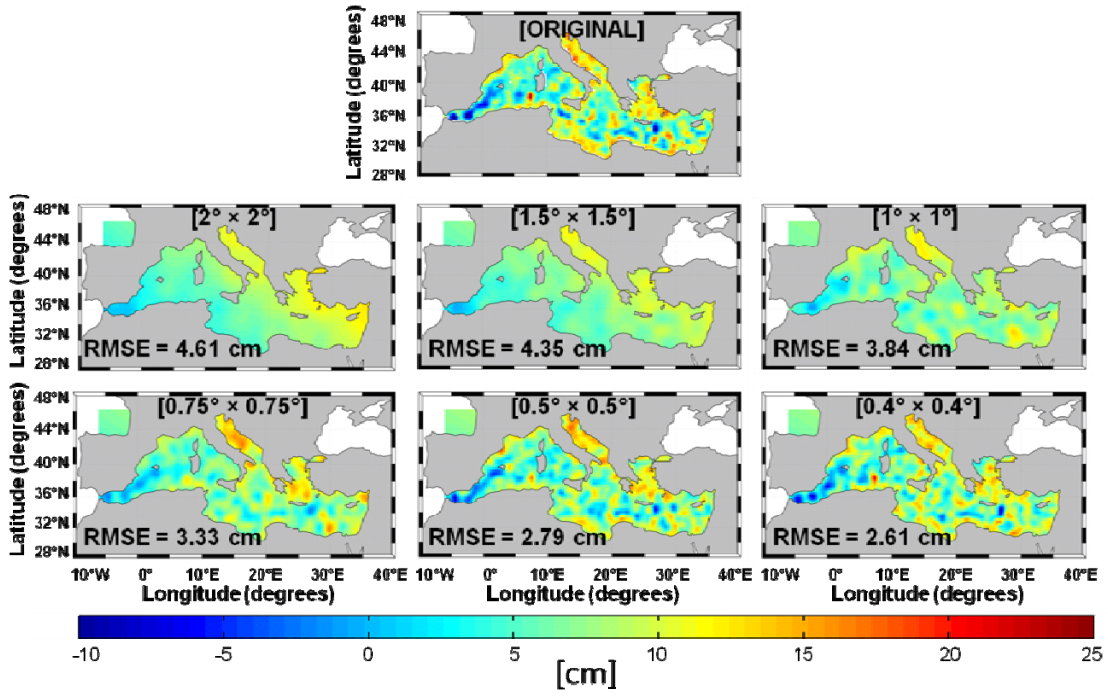
7



1

2 Figure 5: Root mean square errors (cm) associated with the altimetry maps recovered along
3 2014 from the different regular sub-sampled fields mentioned in the text. The black line
4 represents the yearly mean value and the gray patch stands for the annual variability.

5

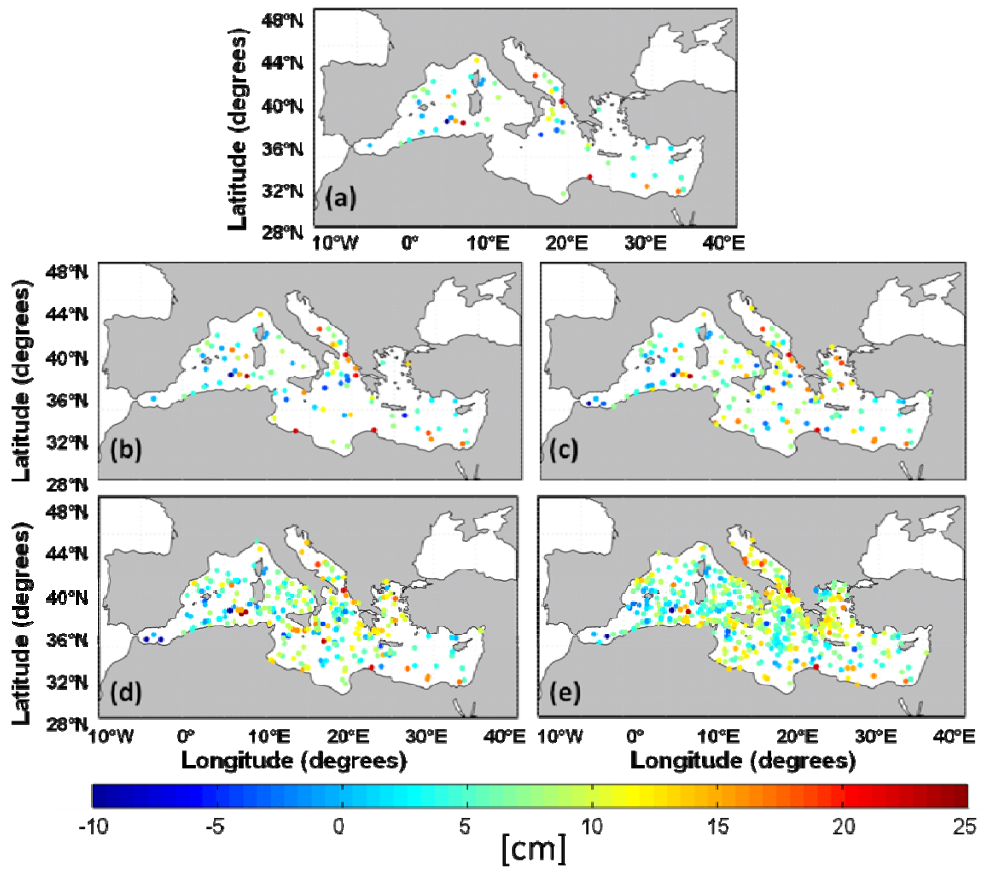


1

2

3 Figure 6: Altimetry maps recovered from the different sub-sampled SLA fields (cm) on
4 December 22, 2014. The spatial resolution of the different regular grids and the RMSEs
5 associated with each reconstruction for that day are also indicated. Moreover, the original SLA
6 field of that day interpolated to a spatial resolution of $\frac{1}{3}^\circ \times \frac{1}{3}^\circ$ is displayed in the uppermost
7 panel for comparison purposes.

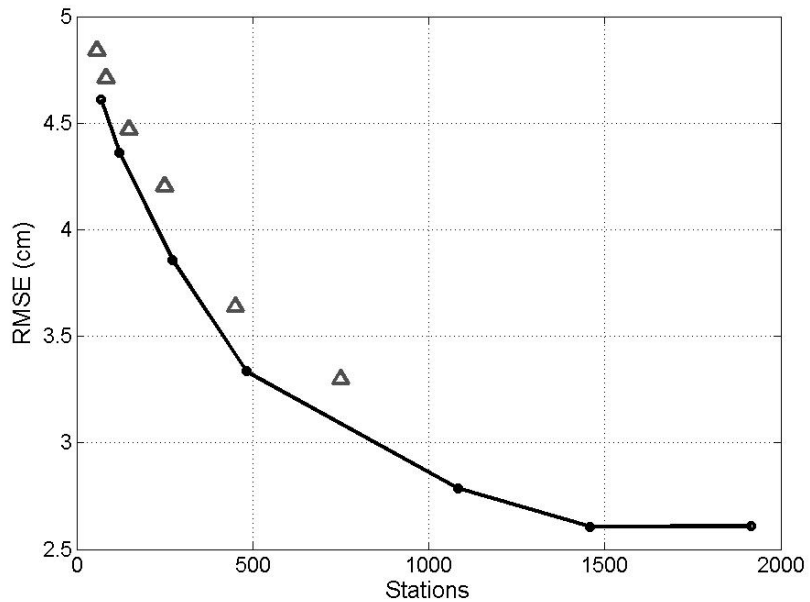
8



1

2 Figure 7: (a) actual positions of the Argo array operating in the Mediterranean basin on
 3 December 22, 2014 (58 floats). Colors indicate the SLA (cm) extracted at those locations from
 4 the original altimetry map of that day. Panels (b), (c), (d), and (e) display the original Argo array
 5 enlarged with random virtual floats in order to simulate an Argo array configuration of 84, 150,
 6 250 and 450 floats, respectively.

7



1

2 Figure 8: Root mean square errors (cm) associated with the altimetry maps recovered on
 3 December 22, 2014 from the different regular sub-sampled fields mentioned in the text (black
 4 line). Triangles stand for the errors associated with the SLA fields retrieved for that day from
 5 the different configurations of the Argo array in the Mediterranean Sea (see Figure 6). Notice
 6 that an Argo array configuration with 750 floats has been also included for comparison
 7 purposes.

8